Electronic Supplementary Information for

Fabrication of Hollow Fibrous Nanosilica with Large Pore Channels

Ngoc Minh Tran,[a] Thang Cao Doan,[a] and Hyojong Yoo[a]*

[a]Department of Materials Science and Chemical Engineering, Hanyang University, Ansan, Gyeonggi-do, 15588, Republic of Korea

E-mail: hjhaha73@hanyang.ac.kr

Experimental section

Reagents

Cetyltrimethylammonium bromide (CTAB, $CH_3(CH_2)_{15}N(CH_3)_3Br$, 99%, Acros Organic), tetraethylorthosilicate (TEOS, 99%, Sigma–Aldrich), 3-(aminopropyl)triethoxysilane (APTES, 98%, Sigma–Aldrich), sodium hydroxide (NaOH, 99%, Sigma–Aldrich), 4-nitrophenol (4-NP, spectrophotometric grade, Sigma-Aldrich), urea ($CO(NH_2)_2$, 98%, Sigma–Aldrich), ammonium hydroxide (NH_4OH, 28–30 wt% ammonia, Sigma–Aldrich), methylene blue solution ($C_{16}H_{18}ClN_3S$, 0.05 wt. % in H_2O, Sigma–Aldrich), 1-pentanol ($CH_3(CH_2)_3CH_2OH$, 98%, Alfa Aesar), cyclohexane (C_6H_{12}, 99%, Sigma–Aldrich), HCl, HNO_3, and purified water were used as purchased without further purification. All the reaction solutions were prepared immediately before the reaction. All of the glassware was washed with aqua regia (concentrated HCl and HNO_3 at a 3:1 volume ratio) before use and thoroughly rinsed with triply distilled water.

Synthesis of dendritic fibrous nanosilica (DFNS)

DFNS was prepared by following a previously reported protocol with slight modifications.[1] TEOS (2.5 g, 0.012 mol) was dissolved in a mixture of cyclohexane (30 mL) and 1-pentanol (1.5 mL). The TEOS precursor solution was added dropwise to an aqueous solution (30 mL) of CTAB (1.0 g, 0.0027 mol) and urea (0.6 g, 0.01 mol). The reaction mixture was vigorously stirred for 2 h at 25 °C, after which it was transferred to a Teflon-lined stainless steel autoclave and kept in a temperature-controlled oven at 120 °C for 6 h. After the mixture naturally cooled to room temperature, the resulting white solids were collected by centrifugation at 3500 rpm for 5 min, washed several times with acetone and deionized (DI) water, and dried at 50 °C for 24 h. The collected powder was calcined at 550 °C for 6 h to obtain DFNS.

Synthesis of spherical nanosilica (*s*-NS)

The *s*-NS was synthesized using the Stöber method with slight differences.[2] In specific, 2.5 g of TEOS (0.012 mol) and 4.60 mL of NH_4OH (aq, 28%) were added to a mixture of ethanol (61.0 mL) and DI water (4.34 mL). After sonication for 30 min, the reaction mixture was stirred at 500 rpm for 12 h at 25 °C. Upon completion of the reaction, the obtained particles were collected by centrifugation (5000 rpm, 5 min), washed several times with ethanol and DI water, and dried at 60 °C for 24 h. The collected powder was heated at 550 °C for 6 h in air.

Synthesis of hollow fibrous nanosilica (HFNS)

An aqueous suspension of DFNS (1.0 mg mL^{-1}, 30 mL) was added to an aqueous solution of NaOH (1.0 M, 30 mL), corresponding to a molar ratio of $NaOH:SiO_2$ = 60:1. The reaction mixture was sonicated for 2 min and then stirred at 500 rpm for 120 min at 25 °C. Next, the resulting HFNS was centrifuged and purified using three repeated cycles of centrifugation (12,000 rpm, 5 min) and re-dispersed in DI water. The obtained HFNS dispersion was dried at 50 °C for 24 h.

The reaction of *s*-NS with NaOH in DI water was conducted using the same procedure used for the synthesis of HFNS, except for the use of *s*-NS in place of DFNS.

Amine functionalization of HFNS and DFNS

HFNS (30 mg) was dispersed in DI water (1 mL) under stirring, to which APTES (0.03 mL) and NH_4OH (aq, 28%) (0.1 mL) were sequentially added. The mixture was continuously stirred for 12 h at 25 °C. The amine-functionalized HFNS product (denoted as $HFNS/NH_2$) was collected by centrifugation (10,000 rpm, 5 min) and rinsed with DI water to remove unreacted APTES. The obtained $HFNS/NH_2$ was re-dispersed in DI water (1 mL) for further use.

The amine functionalization of DFNS (named $DFNS/NH_2$) was performed using the same process as for the preparation of $HFNS/NH_2$, replacing name of HFNS by DFNS.

Synthesis of HFNS/Au and DFNS/Au nanohybrids

HFNS/Au nanohybrids were prepared by modifying our previous protocol.[3] An aqueous suspension of HFNS/NH_2 (30 mg·mL^{-1}, 1 mL) was added to an aqueous solution of $HAuCl_4$ (0.025 M, 0.3 mL) and stirred for 30 min at 25 °C. The obtained product was centrifuged (10,000 rpm, 5 min) and re-dispersed in DI water (1 mL). Afterward, an aqueous solution of $NaBH_4$ (0.1 M, 0.5 mL; maintained in an ice bath) was added to the mixture, which was then stirred for 12 h at 25 °C. Upon completion of the reaction, the resulting HFNS/Au nanohybrids were centrifuged and rinsed with DI water, followed by drying at 50 °C for 12 h prior to use.

The DFNS/Au nanohybrids were prepared using the same procedure as used for the synthesis of HFNS/Au but using DFNS/NH_2 rather than HFNS/NH_2.

Catalysis: 4-nitrophenol (4-NP) reduction

In a typical experiment, a suspension of the as-prepared catalyst (i.e., HFNS/Au or DFNS/Au nanohybrids) in DI water (1 mg·mL^{-1}, 0.025 mL) was added to a mixture of 4-NP (aq) (0.2 mM, 0.85 mL), $NaBH_4$ (aq) (15 mM, 0.5 mL), and DI water (1.4 mL).[4] The reaction mixture was swirled well and transferred to a quartz cuvette. The color of the reaction mixture changed gradually from yellowish to clear as the reaction proceeded. The reaction progress was tracked by monitoring the change in 4-NP peak intensity at regular time intervals (1–2 min) using ultraviolet-visible (UV-vis) spectroscopy. The catalytic activity of DFNS/Au nanohybrids toward 4-NP reduction was studied for comparison.

Characterizations

The glassware was oven-dried prior to use. Powder X-ray diffraction (PXRD) analysis was performed using a RIGAKU Ultima IV diffractometer using Cu-Kα radiation (wavelength 1.5406 Å) in the focused beam configuration at a continuous scan rate of 2 °·min^{-1} in the 5–50° range, at room temperature. The nanoparticles were imaged using scanning electron microscopy (SEM; S-4800, Hitachi). Transmission electron microscopy (TEM) and energy dispersive X-ray (EDX) analyses were performed using a 200-kV Field Emission microscope (JEOL, JEM-2100F). The samples were prepared for TEM by concentrating the nanoparticle mixture through

centrifugation (3 times, 2.30 min, and 9000 rpm), followed by resuspension in ethanol (200 μL) and the immobilization of 1.8 μL portions of the solution on TEM grids (Ted Pella, Inc. Formvar/carbon 400 mesh, copper coated). UV-vis spectra were recorded using a Mega-2100 (Scinco, UV-Vis spectrophotometer). N_2 adsorption isotherms were obtained using a BELSORP-mini II (BEL Japan, Inc.) instrument. High-purity (99.999%) gases were used in the adsorption experiments. All the samples were activated by thorough rinsing, followed by drying under vacuum for 24 h at 25 °C prior to gas sorption measurements.

Table S1. Nitrogen sorption properties of DFNS and HFNS at different reaction times.

Entry	Nanoparticles	Reaction time (min)	S_{BET} (m^2 g^{-1})	Total pore volume (cm^3 g^{-1})	Mean pore diameter (nm)
1	DFNS		318	0.79	9.93
2	HFNS-30min	30	344	1.12	12.78
3	HFNS-60min	60	465	1.48	12.99
4	HFNS-90min	90	507	1.96	15.48
5	HFNS-120min	120	666	2.70	16.22

Table S2. Summary of average particle sizes for *s*-NS before and after reacting with aqueous NaOH for 60, 180, and 300 min.

Entry	Reaction time (min)	Mean diameter (nm)	Number of evaluated particles
1	0	214±13	347
2	60	205±13	107
3	180	204±12	142
4	300	198±10	139

Table S3. Average *s*-NS particle size (without calcination at 550 °C) before and after reacting with aqueous NaOH for 60, 120, and 300 min.

Entry	Reaction time (min)	Mean diameter (nm)	Number of evaluated particles
1	0	216±12	278
2	60	174±13	143
3	180	144±11	168
4	300	115±9	136

Table S4. Rate constants for the reduction of 4-NP catalyzed by HFNS/Au and DFNS/Au, calculated based on the slope of the linear fit of $-\ln(C_t/C_0)$ versus time.

Sample name	Rate constant (10^{-1} min)	Sample name	Rate constant (10^{-1} min)
HFNS/Au_0.025 mg	5.47	DFNS/Au_0.025 mg	1.85
HFNS/Au_0.05 mg	10.76	DFNS/Au_0.05 mg	2.47

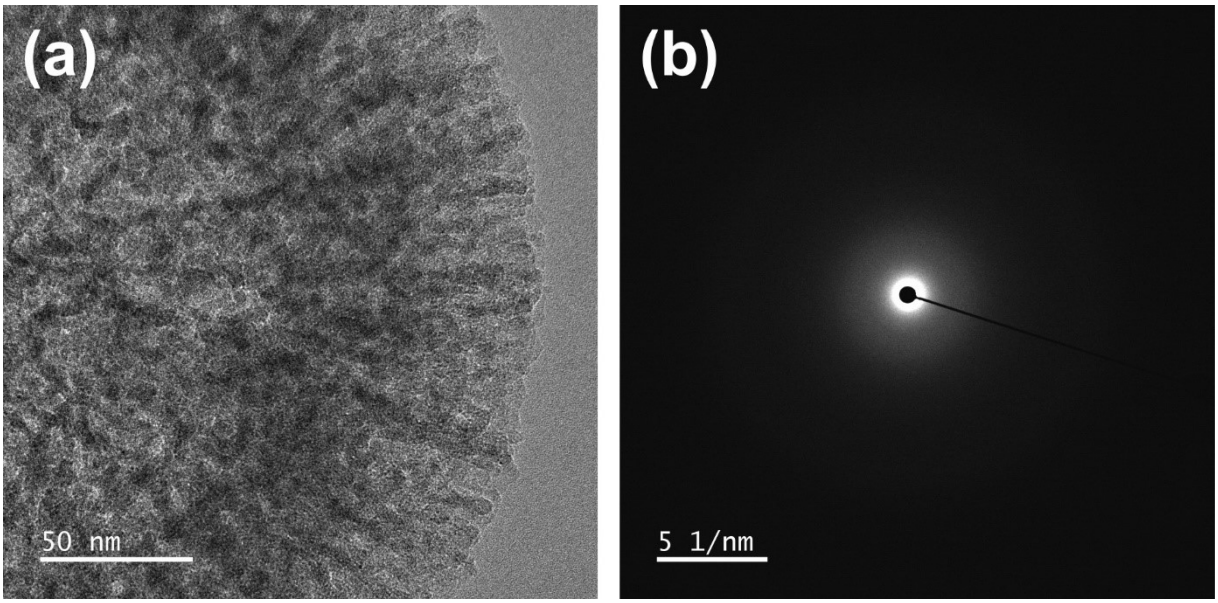

Figure S1. (a) Enlarged TEM image and (b) SAED pattern of HFNS.

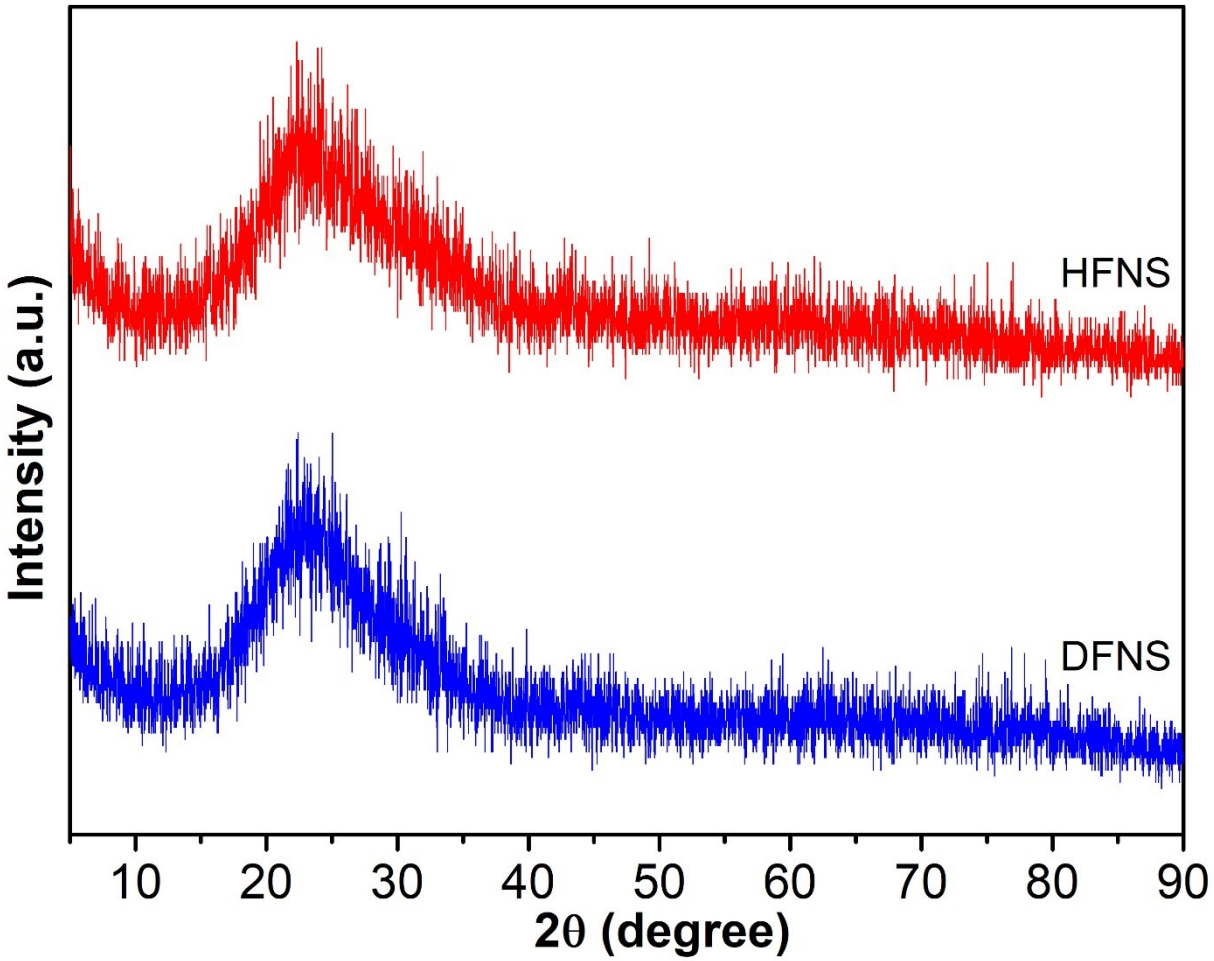

Figure S2. PXRD patterns of DFNS (in blue) and HFNS after etching for 120 min with NaOH solution (in red).

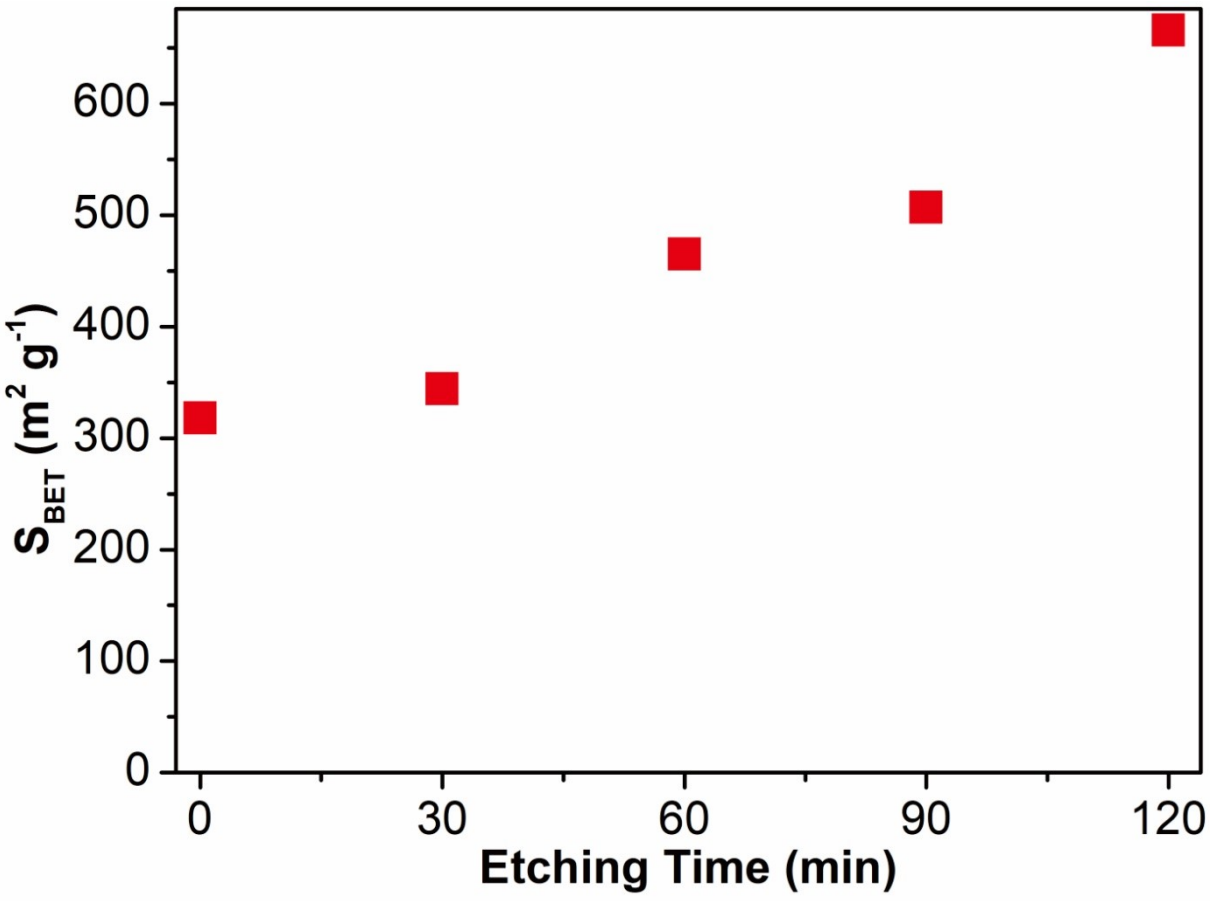

Figure S3. Specific surface area of HFNS as a function of the duration of the reaction between DFNS and NaOH.

The Removal Test of Methylene blue

According to literature, the width of a methylene blue molecule is approximately 9.5 Å,[5] and the length is 13.82 Å or 14.47 Å.[6, 7] The chemical structure of methylene blue is shown below:

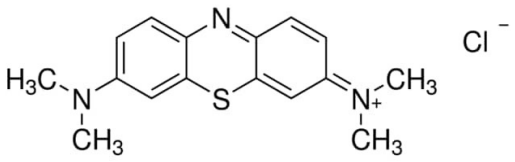

The removal of methylene blue from the aqueous solution using silica-based materials has well investigated.[8-13] Pore size-dependent adsorption of methylene blue by silica materials can be a good test to compare the pore channels of HFNS and those of DFNS. To investigate the adsorption of methylene blue using HFNS and DFNS as adsorbents, we first prepared the calibration curve for methylene blue in an aqueous solution. The concentrations of methylene blue in the solutions are determined by measuring the absorbance at 664 nm by using UV–visible absorption spectrometer.[10] Calibration curve for methylene blue in aqueous solution in this work: $y = 0.1382x$ ($R^2 = 0.995$).

The batch adsorption experiments were performed at 25 °C. Typically, methylene blue solutions (100 mL, 50 mg L^{-1} or 150 mg L^{-1}) was mixed with 100 mg of silica materials (i.e., HFNS and DFNS) to achieve the adsorbent dosage of 1 mg mL^{-1}. The suspension was stirred at 900 rpm. After a designated time interval, the suspension of silica and methylene blue was separated by a centrifugation at 10,000 rpm. The concentration of methylene blue in the obtained solution is checked by UV–visible absorption spectrometer.

The adsorption capacity (Q_e, mg g^{-1}) and removal efficiency (R, %) of methylene blue onto HFNS and DFNS are calculated by the following equations:[14]

$$Q_t = \frac{(C_0 - C_t)V}{m}$$

$$R = \frac{C_0 - C_t}{C_0} \times 100$$

Where C_0 (mg L^{-1}) is the initial concentration of methylene blue

C_t (mg L^{-1}) is the concentration of methylene blue at t minutes

V (L) is the volume of solution

m (g) is the weight of adsorbent used

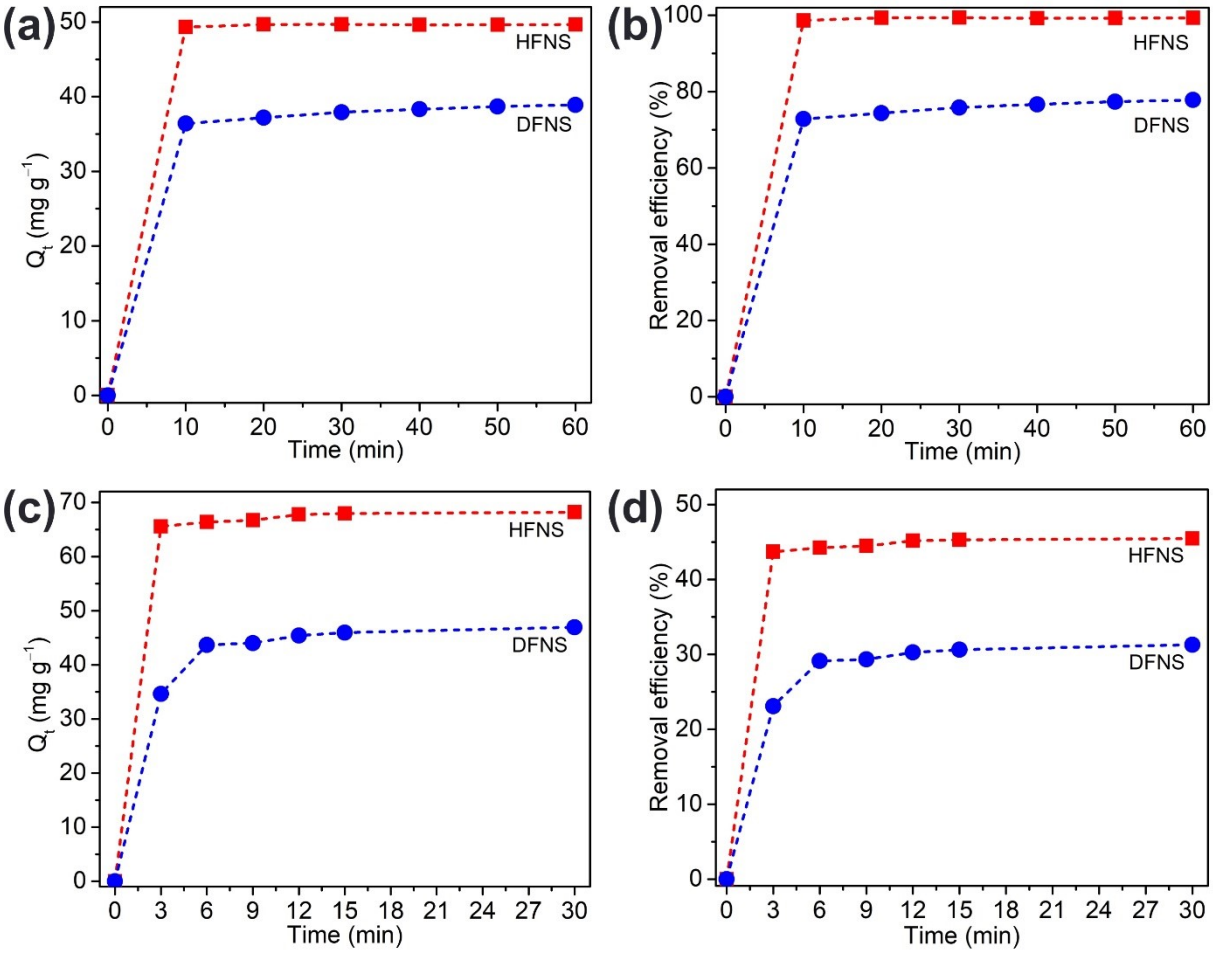

Figure S4. (a, c) Adsorption capacity and (b, d) removal efficiency for methylene blue using HFNS (in red, solid square) and DFNS (in blue, solid circle) as adsorbents (adsorbent dosage of 1 mg mL^{-1}, methylene blue concentration of (a, b) 50 mg mL^{-1} and (c, c) 150 mg mL^{-1}, 25 °C, stirring at 900 rpm).

In Figure S4a, the adsorption of methylene blue by HFNS almost achieves the equilibrium stage after 10 min adsorption with the adsorption capacity of 49.3 mg g^{-1}. After 60 min processing, the adsorption capacity using HFNS adsorbent is 49.7 mg g^{-1}, which is similar to that of 10 min adsorption. In the case of DFNS, with the same protocol, the adsorption capacity for methylene blue after 10 min adsorption is 36.4 mg g^{-1} and it reaches 38.9 mg g^{-1} after 60 min. These data indicate that the adsorption of methylene blue by HFNS is faster than by DFNS: HFNS has higher adsorption capacity than DFNS. It confirms the enhanced activity for methylene blue of HFNS compared to DFNS owing to the larger pore systems of HFNS. In Figure S4b, the methylene blue removal efficiencies of HFNS are 98.6% and 99.3 after 10 min and 60 min adsorption. Meanwhile, the removal efficiencies of DFNS are only 72.8% and 77.8 after 10 min and 60 min adsorption. These data further approve the advantage of HFNS in methylene blue adsorption compared with DFNS.

As shown in Figures S4c and 4d, the adsorption of HFNS for methylene blue nearly archives equilibrium after only 3 min with the adsorption capacity and removal efficiency of 65.5 mg g^{-1} and 43.7%. Meanwhile, in the case of DFNS, after 3 min adsorption, the adsorption capacity and removal efficiencies are 34.4 mg g^{-1} and 23.1%. In addition, compared to HFNS, the adsorption process of DFNS for methylene blue to reach equilibrium is slower (6 min) with the adsorption capacity and removal efficiency of 43.7 mg g^{-1} and 29.1%.

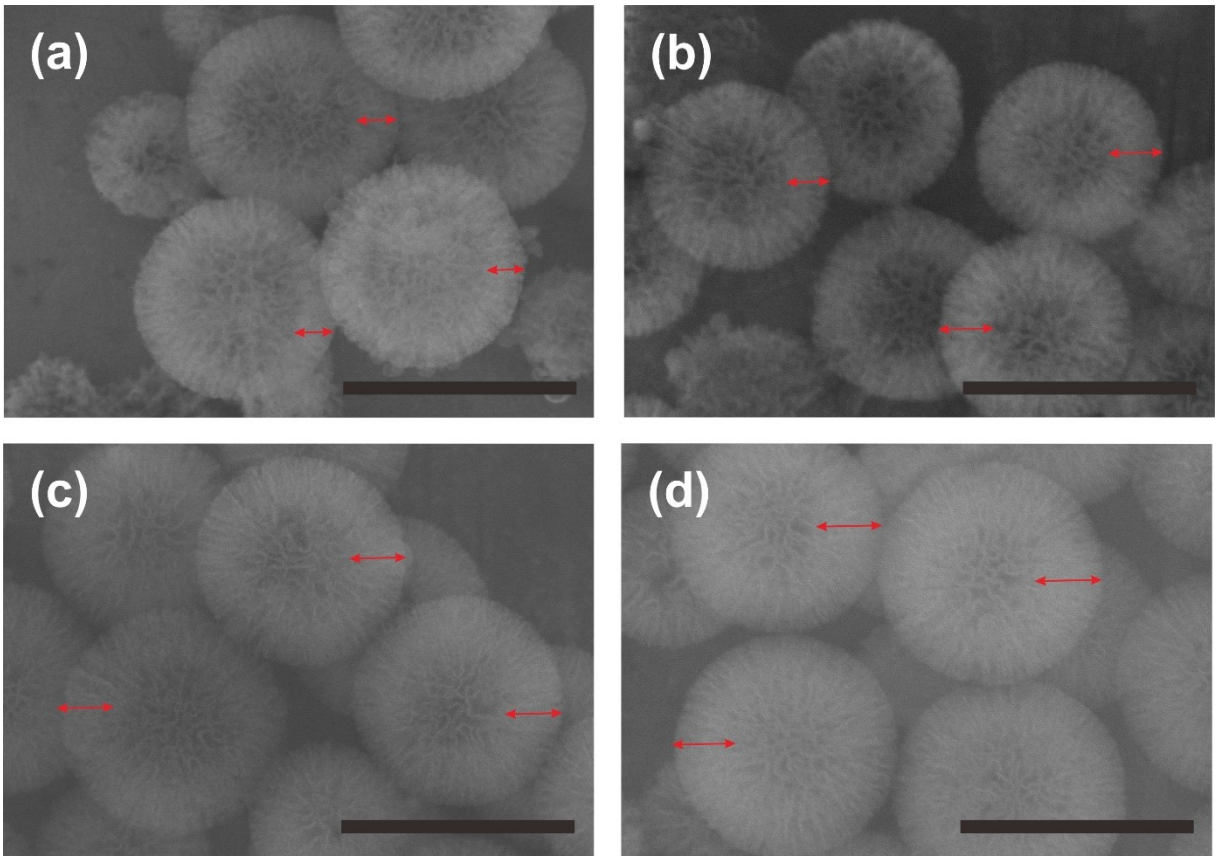

Figure S5. SEM images of HFNS samples obtained at different NaOH concentrations: (a) 0.8 M, (b) 0.5 M, (c) 0.4 M, and (d) 0.1 M (for 120 min), Scale bars: 500 nm.

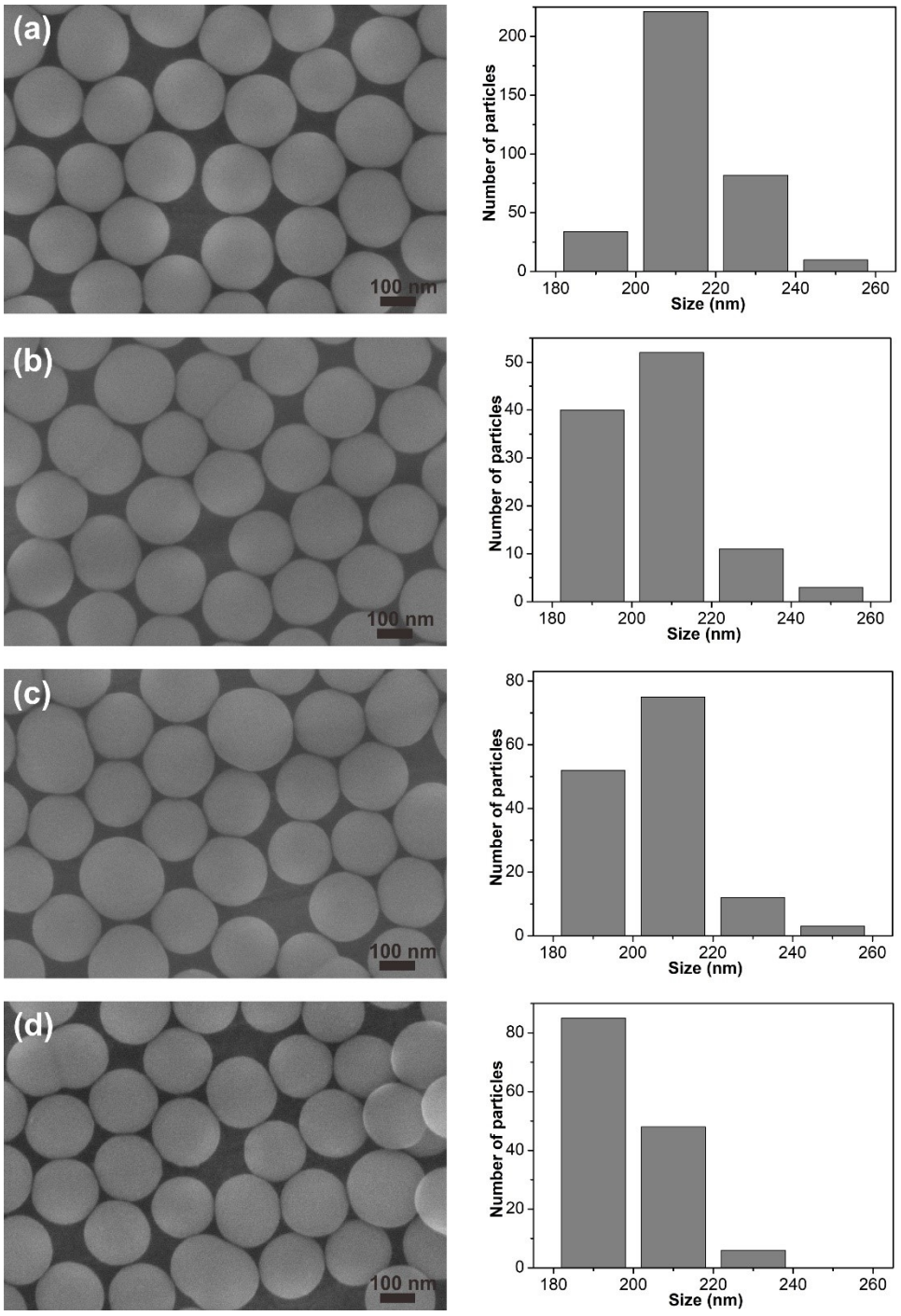

Figure S6. SEM images and corresponding size distributions of *s*-NS (a) before and (b, c, d) after reacting for (b) 60 min, (c) 180 min, and (d) 300 min. Scale bar: 100 nm.

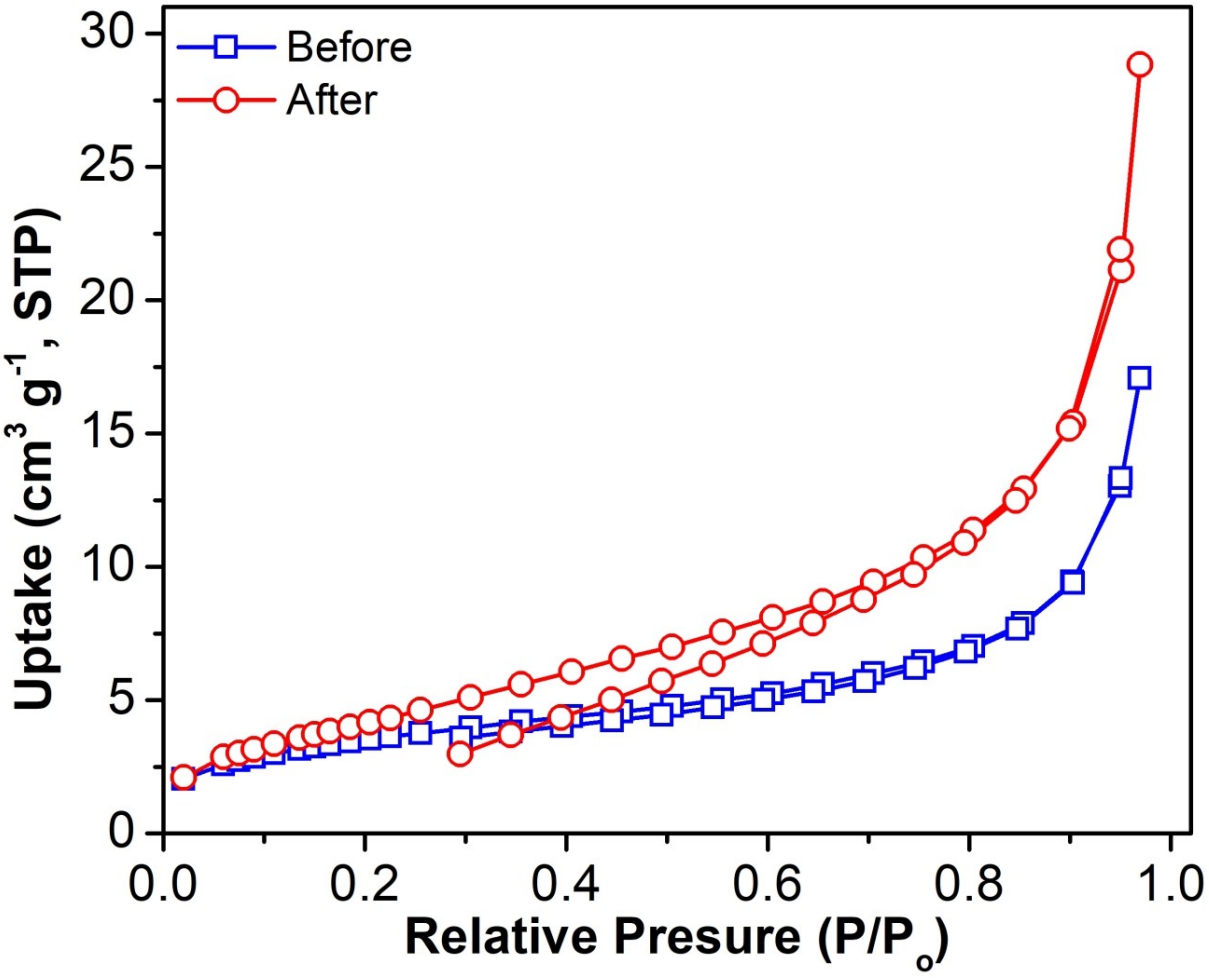

Figure S7. Nitrogen sorption of *s*-NS measured at 77 K before (in blue) and after (in red) the reaction with NaOH solution for 120 min.

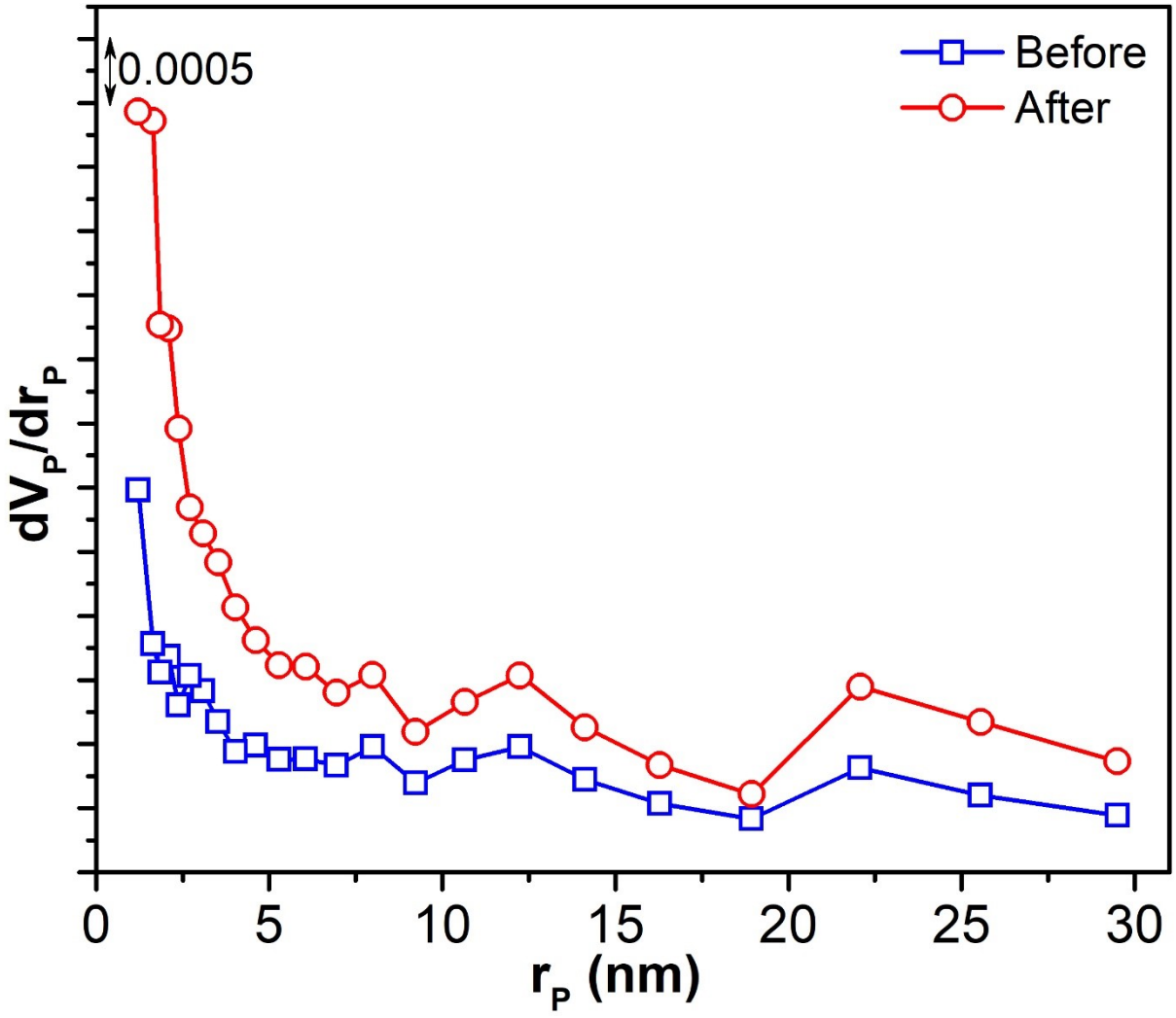

Figure S8. Pore size distributions of *s*-NS before (in blue) and after (in red) the reacting with NaOH solution for 120 min.

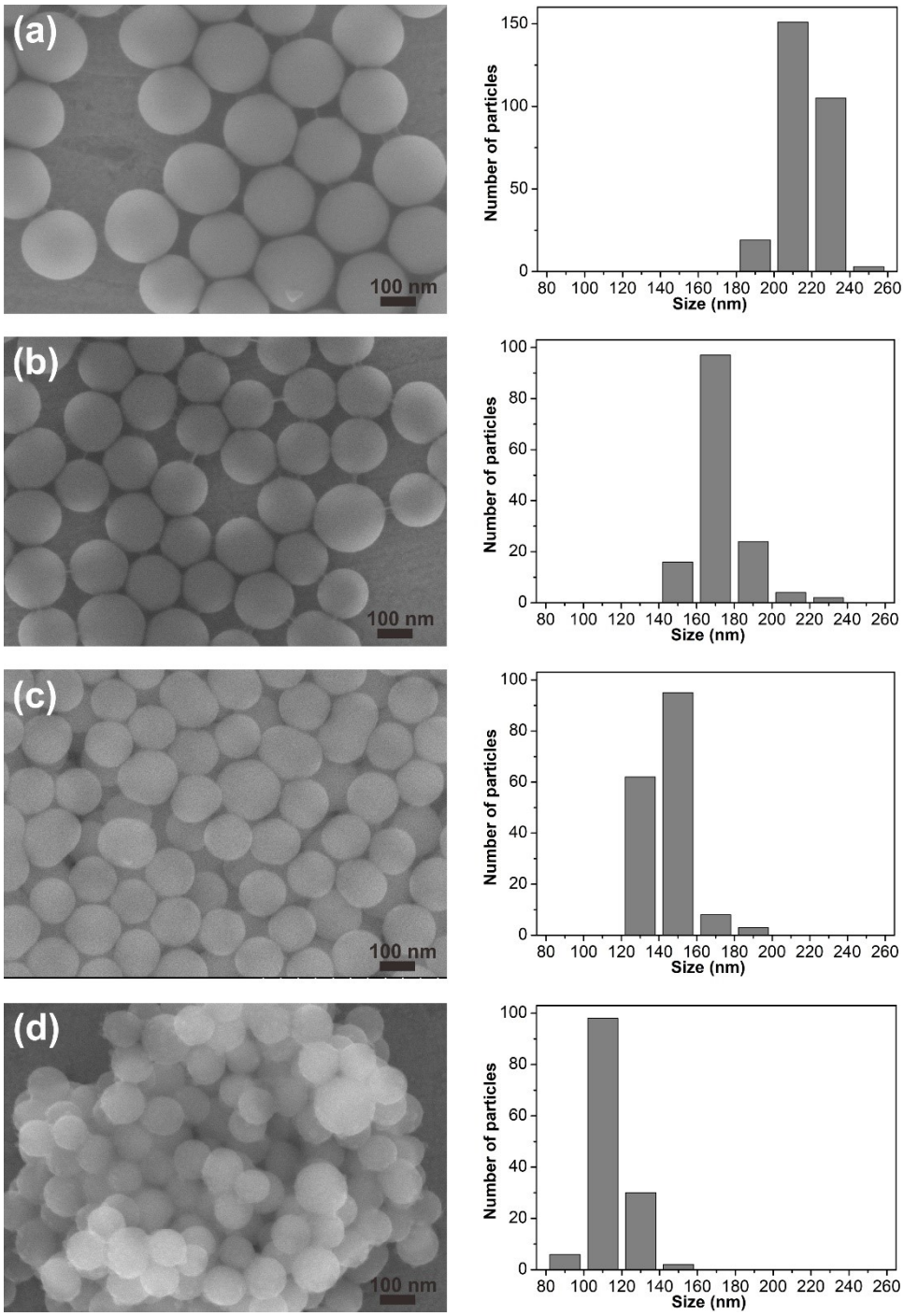

Figure S9. SEM images and corresponding size distributions of *s*-NS (without heating at 550 °C) (a) before and (b, c, d) after reacting for (b) 60 min, (c) 180 min, and (d) 300 min. Scale bar: 100 nm.

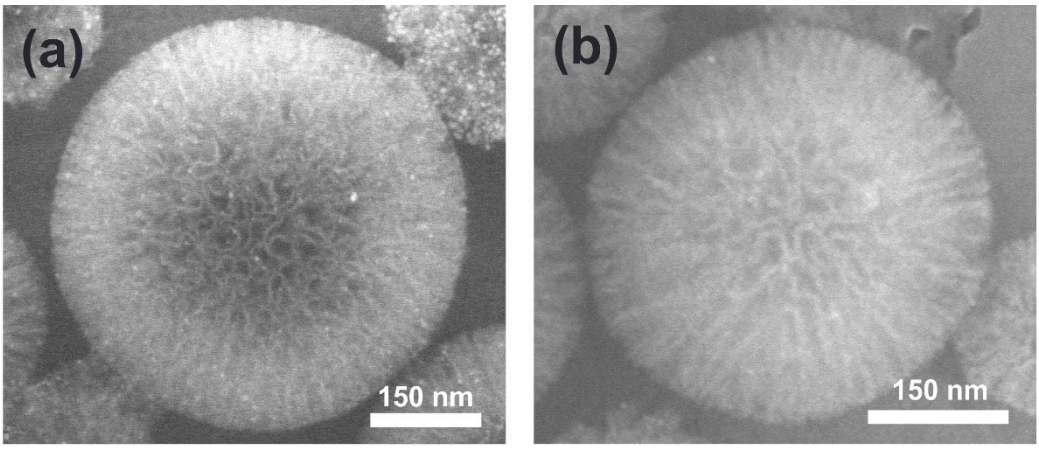

Figure S10. SEM images of (a) HFNS/Au nanohybrids and (b) DFNS/Au nanohybrids.

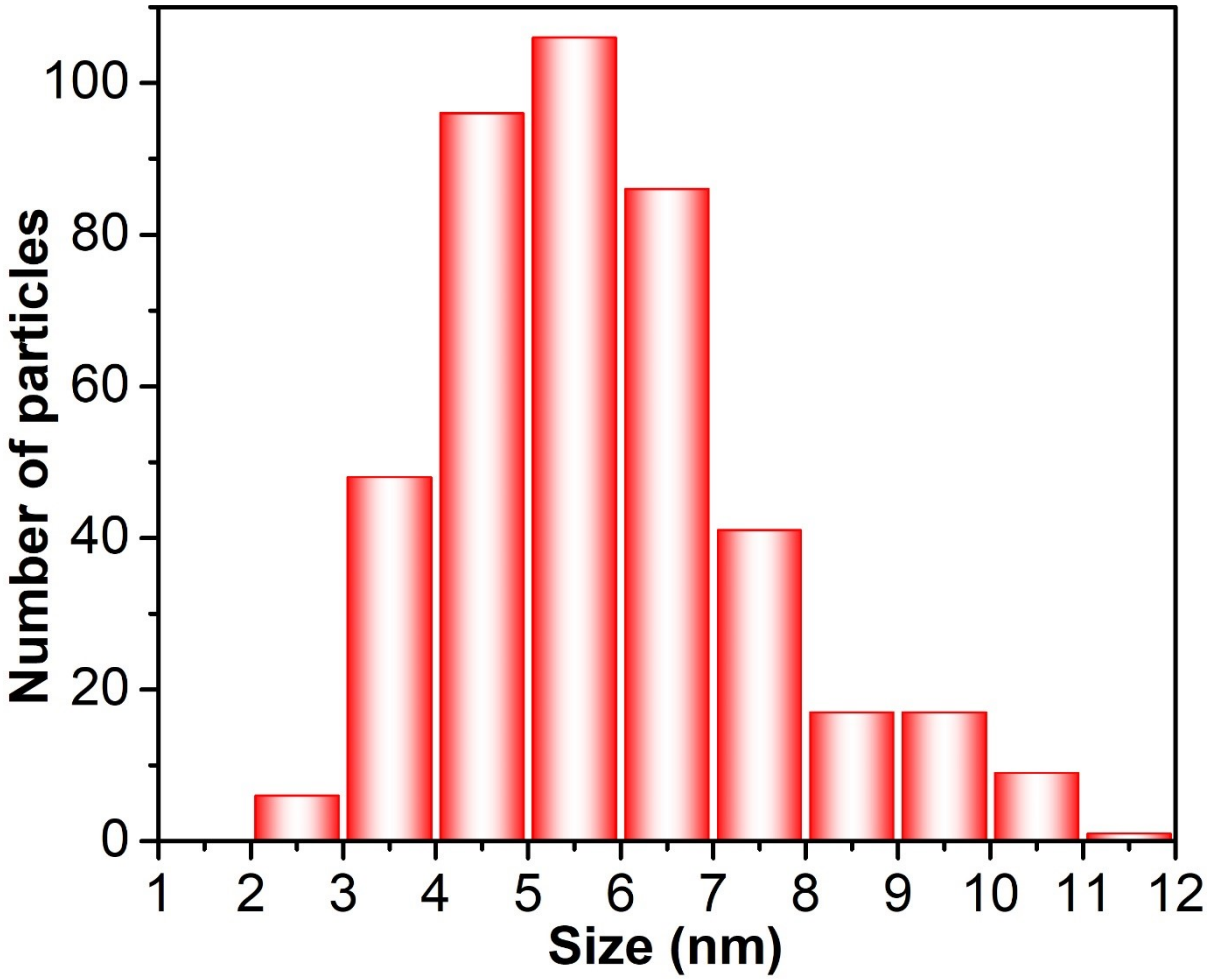

Figure S11. Size (diameter) distribution of Au nanoparticles in HFNS/Au.

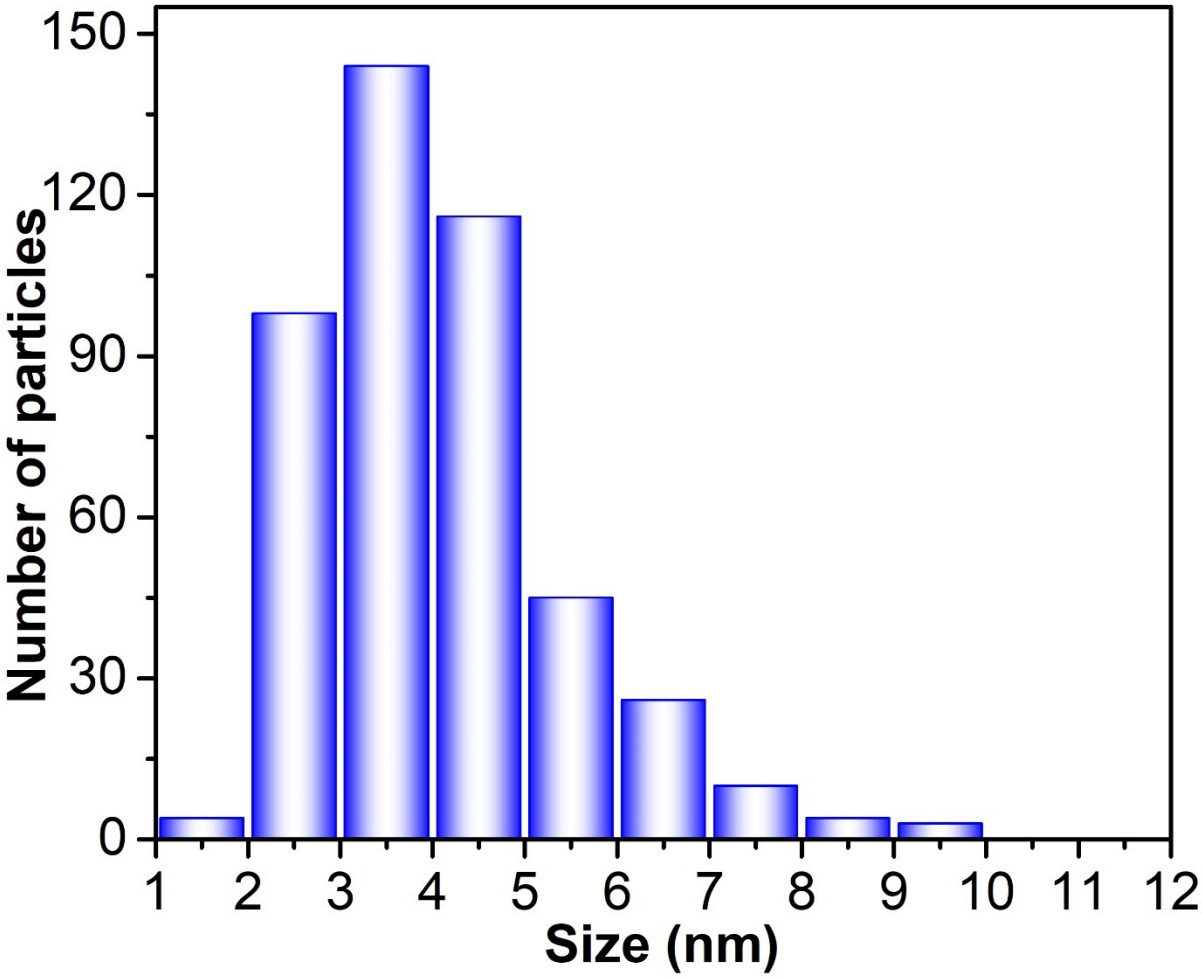

Figure S12. Size (diameter) distribution of Au nanoparticles in DFNS/Au.

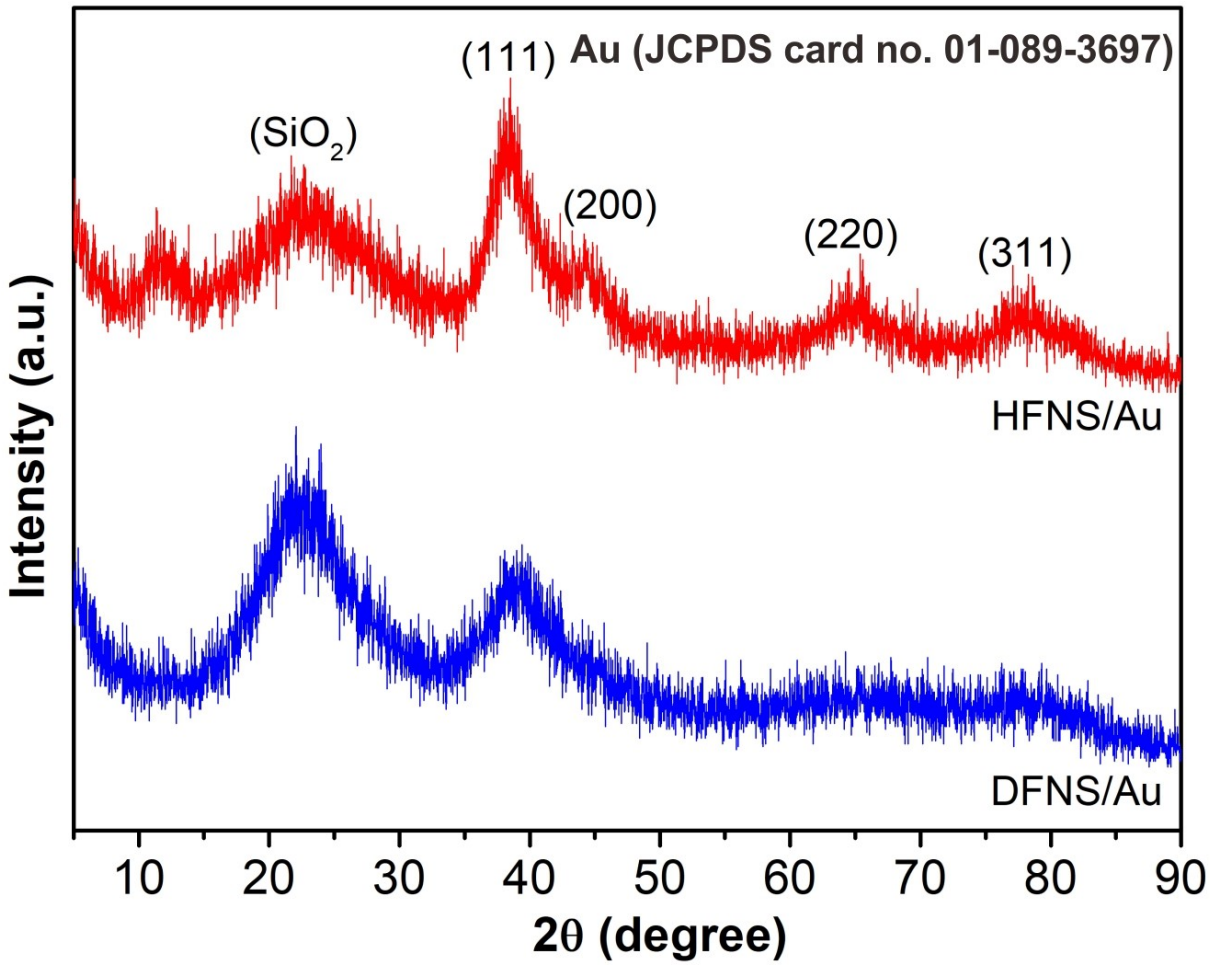

Figure S13. XRD patterns of HFNS/Au (in red) and DFNS/Au (in blue).

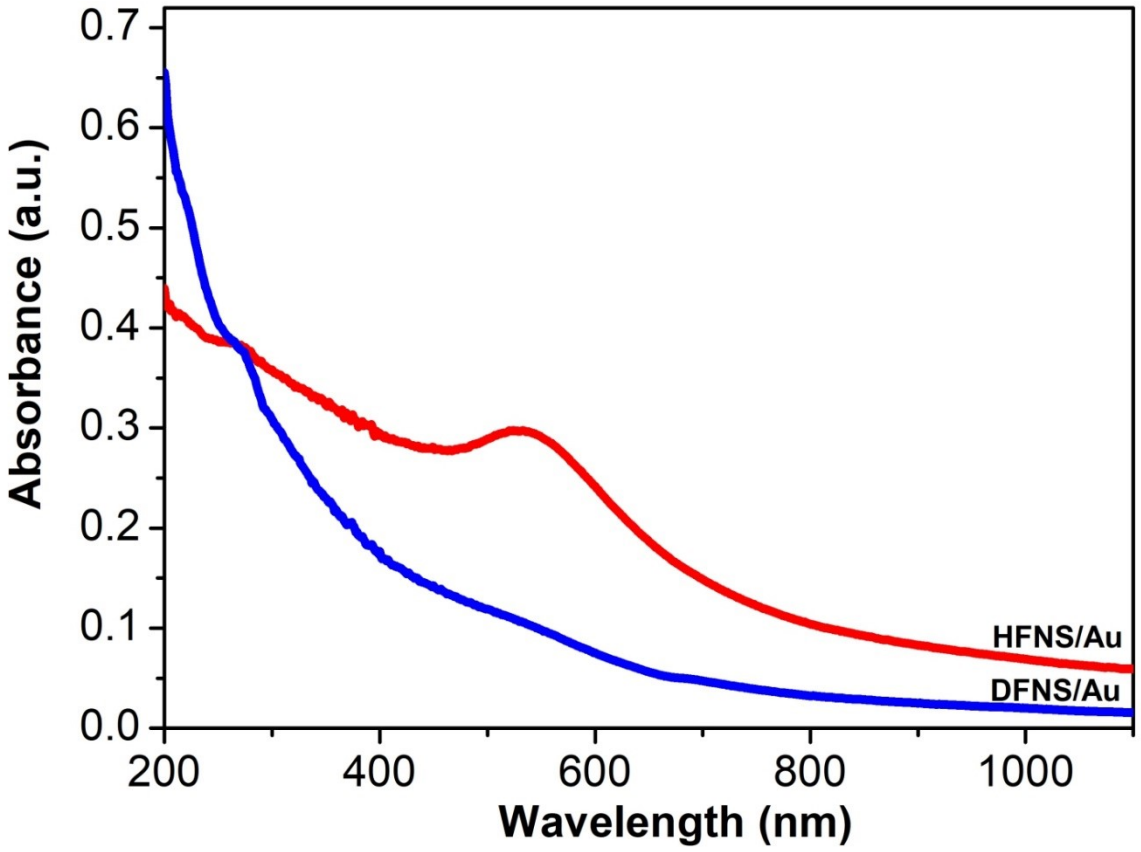

Figure S14. UV-Vis spectra of HFNS/Au (in red) and DFNS/Au (in blue).

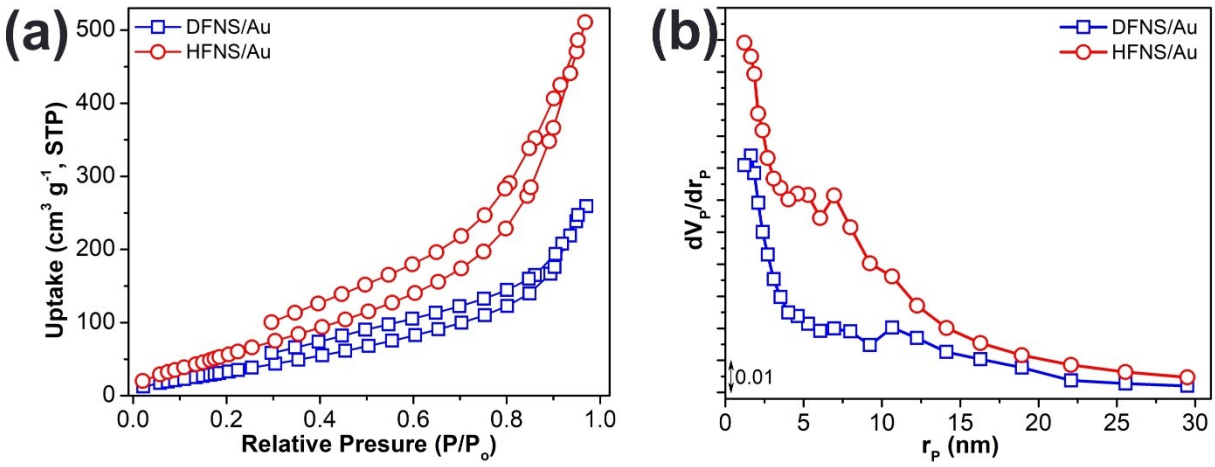

Figure S15. (a) Nitrogen sorption measured at 77 K and (b) pore size distributions for HFNS/Au (in red, -○-) and DFNS/Au (in blue, -□-).

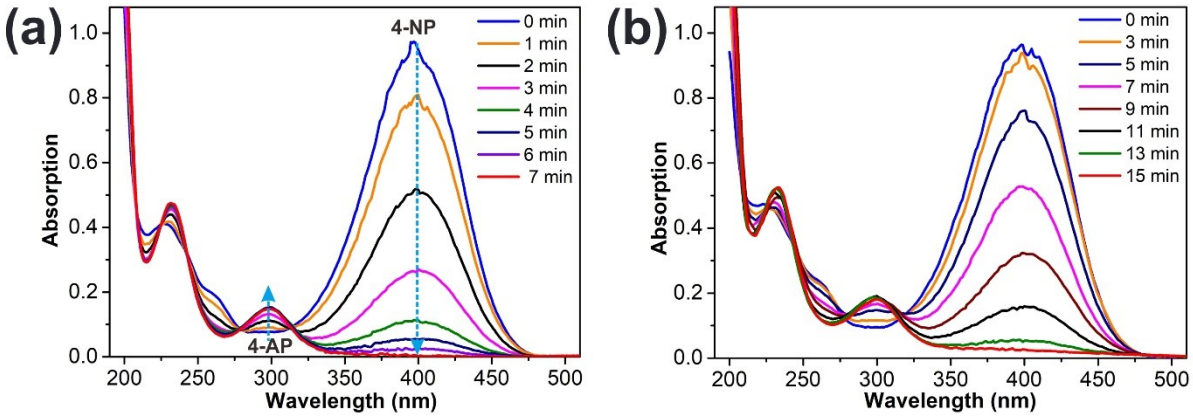

Figure S16. Time-dependent UV-Vis spectra of the reduction of 4-NP catalyzed by (a) HFNS/Au and (b) DFNS/Au with 0.025 mg catalyst dosage. Catalysts were dispersed in DI water (1 mg·mL^{-1}) prior to use.

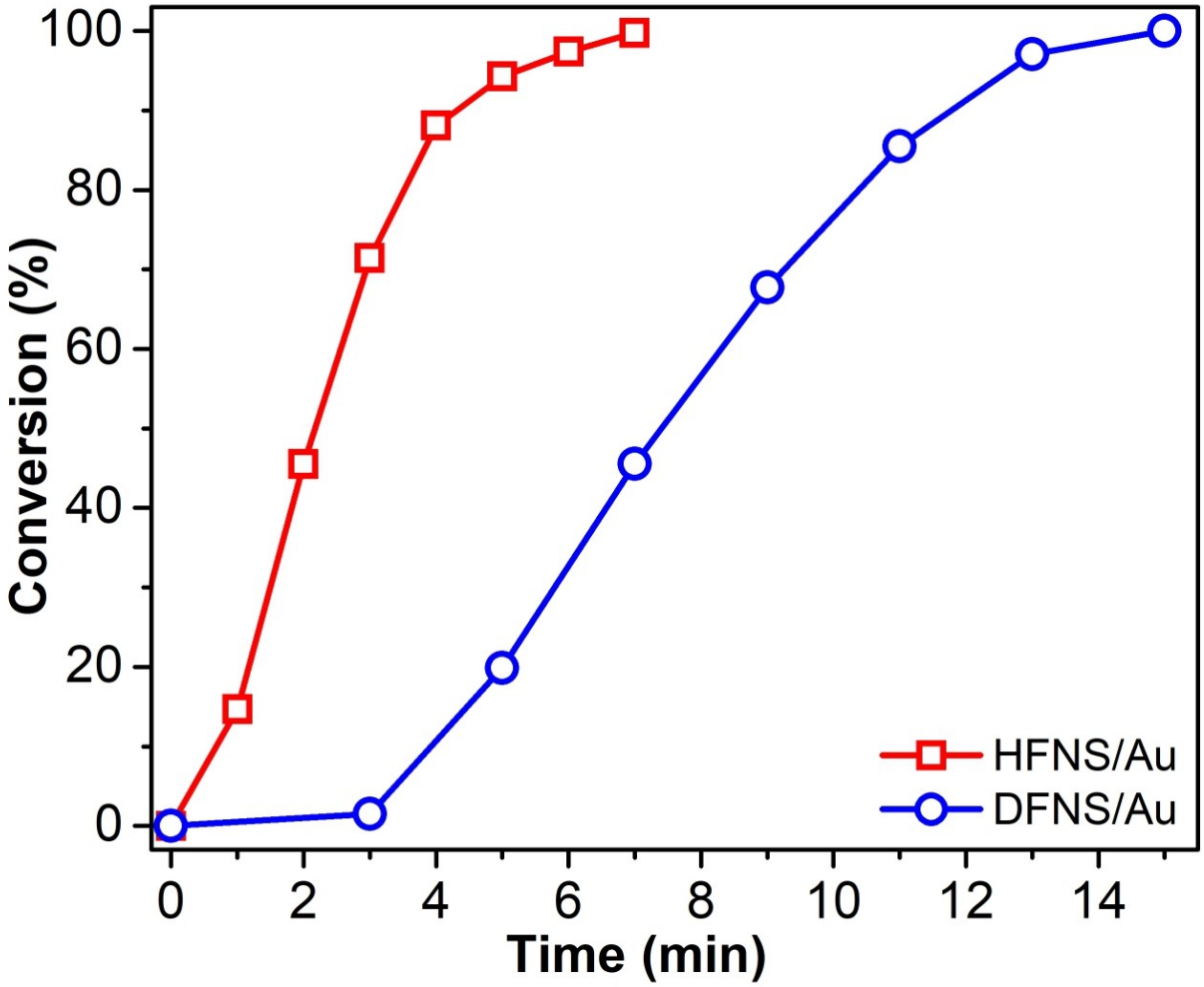

Figure S17. 4-NP conversion by HFNS/Au (in red, empty square) and DFNS/Au (in blue, empty circle) catalysts at dosage of 0.025 mg. 4-NP conversion was calculated as follows: Conversion (%) = $(1 - C_t C_0^{-1}) \times 100$, where C_t is the absorption of 4-NP at a given reaction time (t), and C_0 is the initial absorption by 4-NP at $t = 0$.

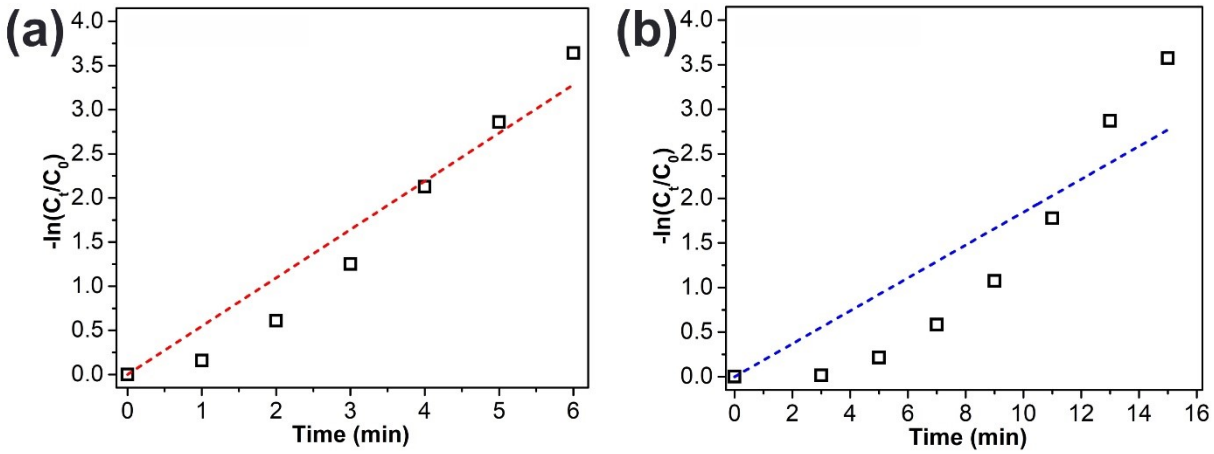

Figure S18. Plot of $-\ln(C_t/C_0)$ versus time for the reduction of 4-NP with (a) HFNS/Au and (b) DFNS/Au catalyst, at the dosage of 0.025 mg.

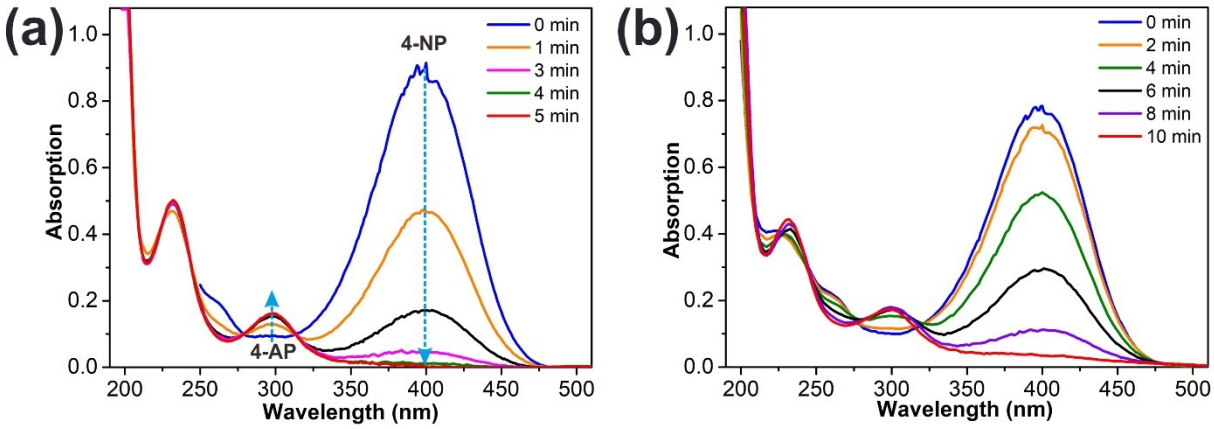

Figure S19. Evolution of UV-Vis spectra of 4-NP reduction catalyzed by (a) HFNS/Au and (b) DFNS/Au at a 0.050 mg catalyst dosage.

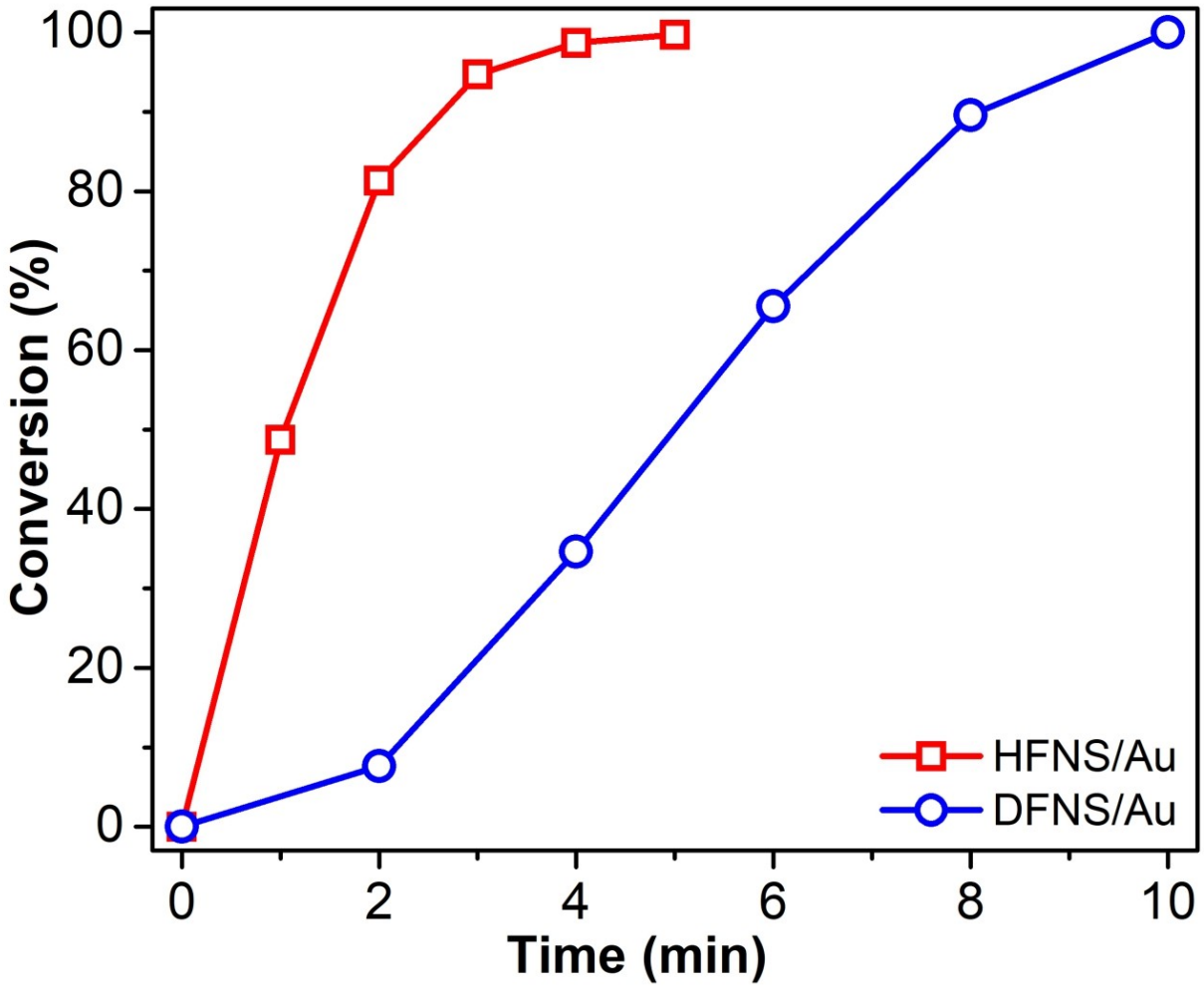

Figure S20. 4-NP conversion by HFNS/Au (in red, open square) and DFNS/Au (in blue, open circle) catalysts at a dosage of 0.050 mg. 4-NP conversion was calculated as follows: Conversion (%) = $(1 - C_t C_0^{-1}) \times 100$, where C_t is the absorption of 4-NP at a given reaction time (t), and C_0 is the initial absorption of 4-NP at $t = 0$. The data indicate that the reduction of 4-NP is faster when using HFNS/Au catalyst compared to DFNS/Au.

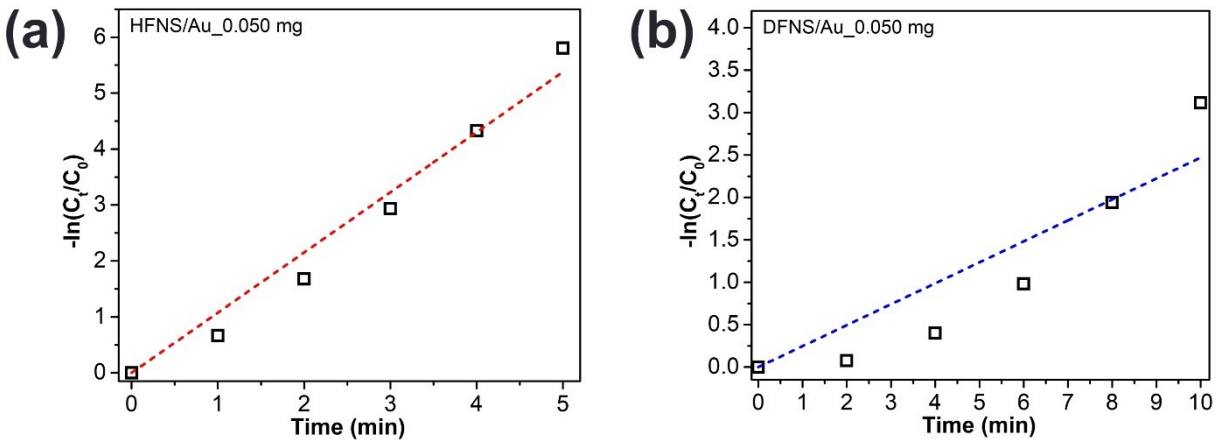

Figure S21. Plot of $-\ln(C_t/C_0)$ versus time for the reduction of 4-NP with (a) HFNS/Au and (b) DFNS/Au catalyst, at the dosage of 0.050 mg. The reduction time and rate constant for HFNS/Au and DFNS/Au are 5 min and 10.76×10^{-1} min^{-1} and 10 min and 2.47×10^{-1} min^{-1}, respectively.

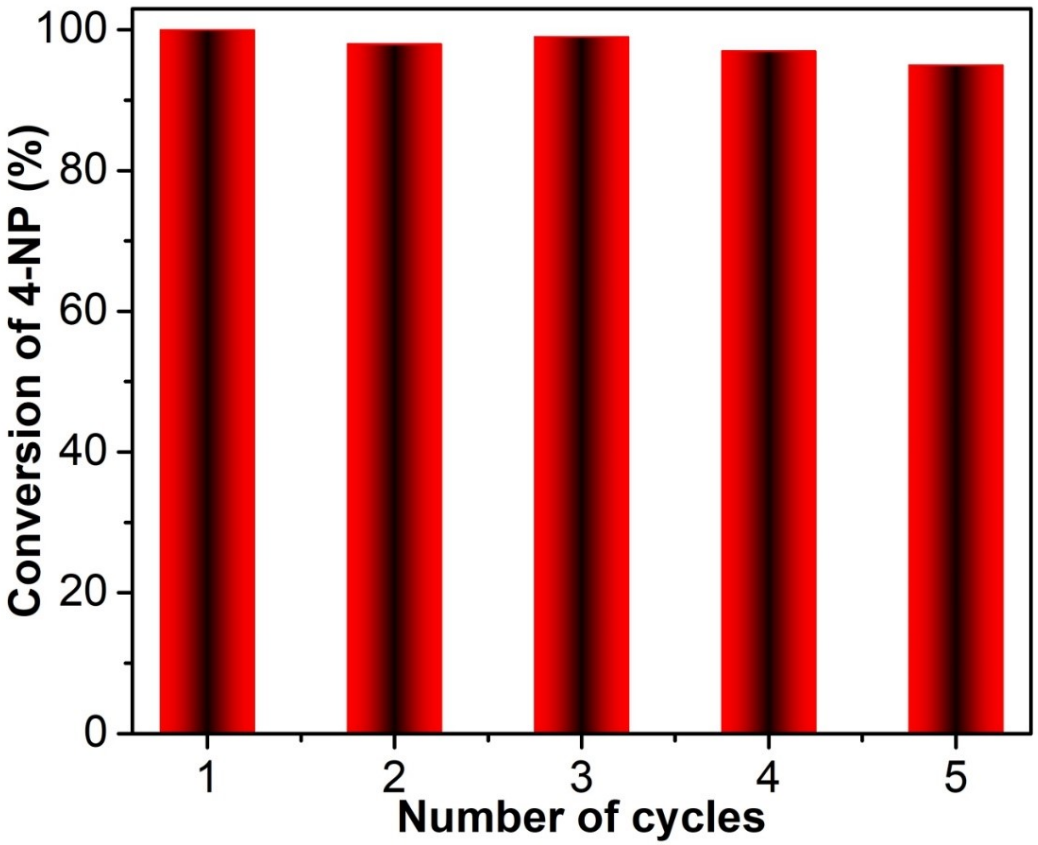

Figure S22. Recycling performance of HFNS/Au catalyst based on the conversion of 4-NP.

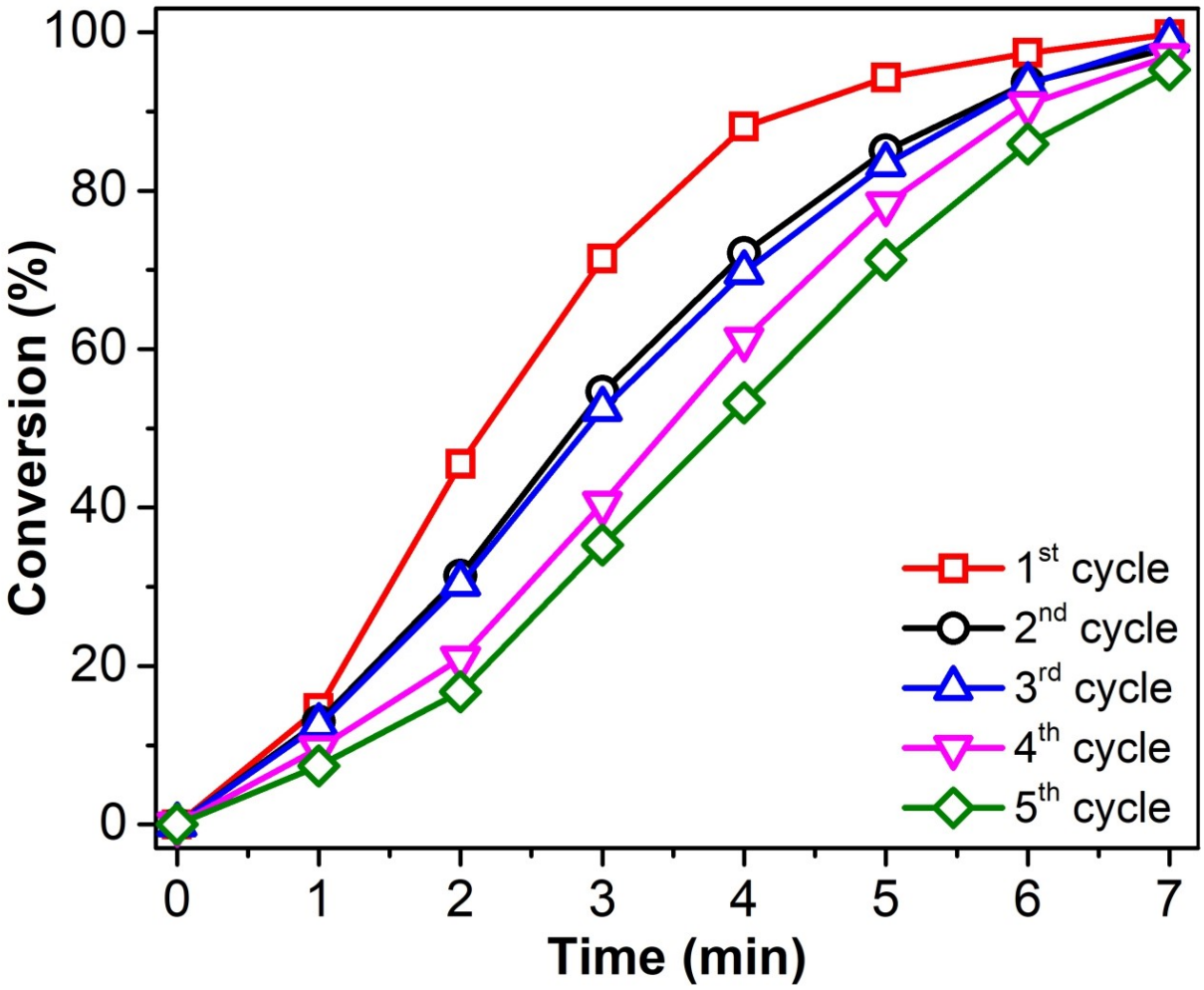

Figure S23. 4-NP conversion for the recycling performance of the HFNS/Au catalyst. 4-NP conversion was calculated as follows: Conversion (%) = $(1 - C_t C_0^{-1}) \times 100$, where C_t is the absorption of 4-NP at a given reaction time (t), and C_0 is the initial absorption of 4-NP at $t = 0$.

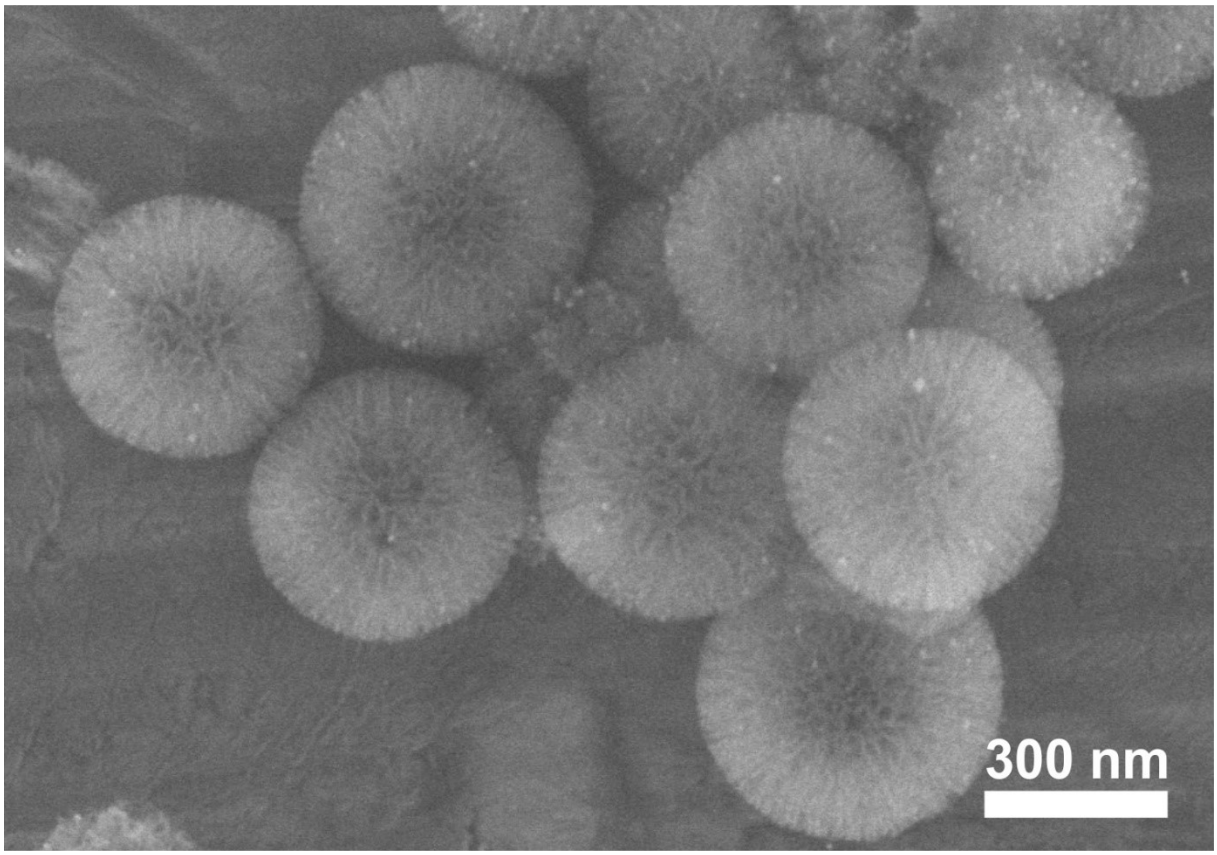

Figure S24. SEM image of HFNS/Au after recycling (five cycles). Scale bar: 300 nm.

Reference

1. W. Byoun, S. Jung, N. M. Tran and H. Yoo, *ChemistryOpen*, 2018, **7**, 349-355.
2. W. Stöber, A. Fink and E. Bohn, *J. Colloid Interface Sci.*, 1968, **26**, 62-69.
3. N. M. Tran, S. Jung and H. Yoo, *Nano Res.*, 2020, **13**, 775-784.
4. N. M. Tran, H. D. Mai and H. Yoo, *Nano Res.*, 2018, **11**, 5890-5901.
5. P. Jia, H. Tan, K. Liu and W. Gao, *Journal*, 2018, **8**.
6. J. d. S. Macedo, N. B. da Costa Júnior, L. E. Almeida, E. F. d. S. Vieira, A. R. Cestari, I. d. F. Gimenez, N. L. Villarreal Carreño and L. S. Barreto, *J. Colloid Interface Sci.*, 2006, **298**, 515-522.
7. G. L. Dotto, J. M. N. Santos, I. L. Rodrigues, R. Rosa, F. A. Pavan and E. C. Lima, *J. Colloid Interface Sci.*, 2015, **446**, 133-140.
8. G. Mitchell, P. Poole and H. D. Segrove, *Nature*, 1955, **176**, 1025-1026.
9. K. Gude, V. M. Gun'ko and J. P. Blitz, *Colloids Surf., A*, 2008, **325**, 17-20.
10. M. M. Ayad, A. Abu El-Nasr and J. Stejskal, *J. Ind. Eng. Chem.*, 2012, **18**, 1964-1969.
11. V. Russo, D. Masiello, M. Trifuoggi, M. Di Serio and R. Tesser, *Chem. Eng. J.*, 2016, **302**, 287-295.
12. Y. Li, S. Wang, Z. Shen, X. Li, Q. Zhou, Y. Sun, T. Wang, Y. Liu and Q. Gao, *ACS Omega*, 2020, **5**, 28382-28392.
13. X. Han, Y. Wang, N. Zhang, J. Meng, Y. Li and J. Liang, *Colloids Surf., A*, 2021, **617**, 126391.
14. M. Sari Yilmaz, *Microporous Mesoporous Mater.*, 2022, **330**, 111570.